ACS OMEGA

http://pubs.acs.org/journal/acsodf

Article

Comparative Analysis of Metabolic Compositions and Trace Elements of *Ornithogalum caudatum* with Different Growth Years

Xueliang Zhao, Guangyu Lin, Tong Liu, Xue Zhang, and Yang Xu*

Cite This: *ACS Omega* 2023, 8, 23889−23900

Read Online

ACCESS | Metrics & More | Article Recommendations | Supporting Information

ABSTRACT: As a traditional medicine with extensive history, *Ornithogalum caudatum* has high nutritional and medicinal value. However, its quality evaluation criteria are insufficient because it is not included in the pharmacopeia. Simultaneously, it is a perennial plant, and the medicinal ingredients change with the growth years. Currently, studies on the synthesis and accumulation of metabolites and elements in *O. caudatum* during different growth years are unavailable. To address this issue, in this study, the 8 main active substances, metabolism profiles, and 12 trace elements of *O. caudatum* from different growth years (1, 3, and 5 years old) were analyzed. The main substances of *O. caudatum* changed significantly in different years of growth. Saponin and sterol contents increased with age; however, the polysaccharide content decreased. For metabolism profiling, ultrahigh-performance liquid chromatography tandem mass spectrometry was performed. Among the three groups, 156 differential metabolites with variable importance in projection values >1.0 and $p < 0.05$ were identified. Among the differential metabolites, 16 increased with increasing years of growth and have the potential to become age-identified markers. A trace element study showed that the contents of K, Ca, and Mg were higher, and the ratio of Zn/Cu was less than 0.1%. Heavy metal ions in *O. caudatum* did not increase with age. The results of this study provide a basis to evaluate the edible values of *O. caudatum* and facilitate further exploitation.

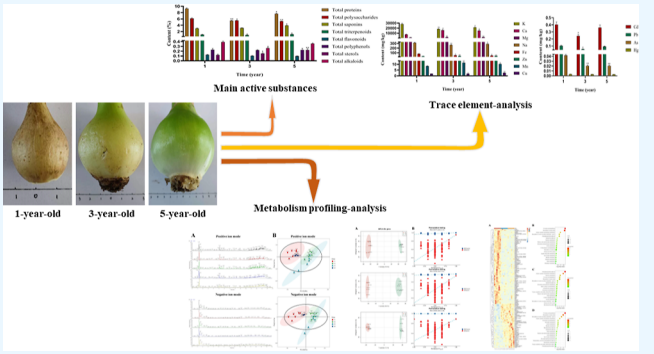

1. INTRODUCTION

Ornithogalum caudatum Jacq. is a perennial herb of *Ornithogalum* in *Liliaceae*. *O. caudatum* is native to southern Africa and is mainly distributed in the temperate regions of the Eastern Hemisphere.[1] In the mid-20th century, *O. caudatum* was introduced to China as an ornamental plant and is now widely cultivated in Jilin, Guangdong, and other regions.[2] *O. caudatum* has high ornamental and medicinal value.[3] Initially, fishermen discovered that it could treat swelling, pain, and inflammation.[4] Later, it was mostly used for external applications to treat furuncles, swelling, and pain and was administered orally for the treatment of hepatitis and liver cancer.[5] *O. caudatum* contains several active compounds, including saponins, polysaccharides, flavonoids, and terpenoids.[6,7] It has various pharmacological effects,[8−10] such as antitumor, liver protection, immune enhancement, anti-inflammatory, pain relief, and antioxidation.

However, owing to the short medicinal history of *O. caudatum*, its quality evaluation criteria are insufficient. Currently, quality evaluation is based on local standards, such as DB22/T 3142-2020, and only the saponin and polysaccharide contents have been determined. Furthermore, as a perennial herb, the accumulation and composition of its metabolites vary with growth years.[11] There have been no studies on the variation of metabolites of *O. caudatum* with growth time. Therefore, exploring the variation in metabolites over time is of great significance for meeting the particular requirements of enterprises, for example, enterprises that plan to use *O. caudatum* saponins to develop antitumor drugs. Other enterprises may require flavonoids from *O. caudatum* to develop antioxidant health products. Therefore, exploring metabolite changes over time is important to formulate a reasonable harvest period.

Metabolomics is an emerging discipline that developed rapidly in the mid-1990s and is an important part of systems biology research.[12,13] It aims to detect the overall trajectory of endogenous metabolites in organisms or cells under specific conditions to reflect the pathological and physiological processes of organisms. Some differential metabolites detected have become potential markers that characterize the pathological and physiological states of organisms.[14,15] Recently, metabolomics has been widely used in comparative

Received: April 6, 2023
Accepted: June 8, 2023
Published: June 21, 2023

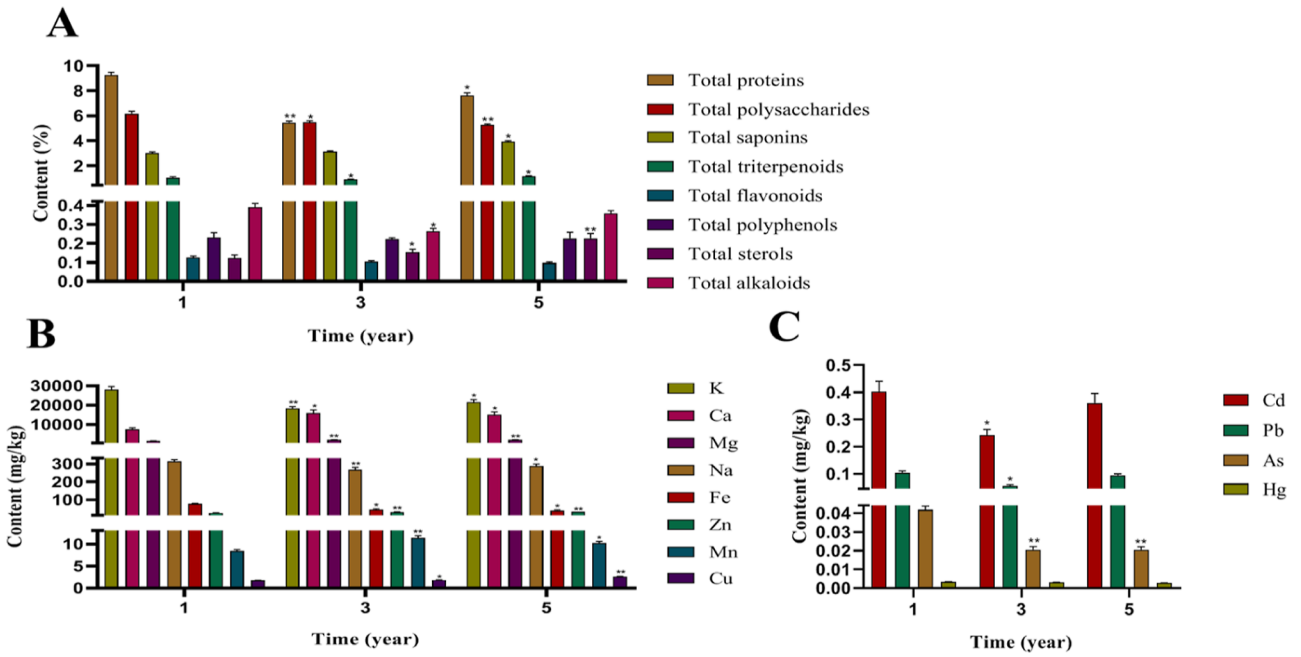

Figure 1. Changes in main active substances and trace elements in *O. caudatum* with growth years. (A) Changes in total saponins, total polysaccharides, total proteins, total flavonoids, total polyphenols, total triterpenoids, total steroids, total alkaloids, and total sterols; (B) contents of K, Ca, Mg, Na, Fe, Zn, Mn, and Cu; and (C) contents of harmful metals (Cd, Pb, As, and Hg). *$p < 0.05$ and **$p < 0.01$ compared with 1 year old *O. caudatum*.

studies of metabolites from different sources, varieties, and growth stages.[16,17] These studies have great significance in identifying the different utilization potentials of medicinal plants and growth regulation markers. For example, Xue et al.[18] analyzed and compared the chemical constituents of *Polygala tenuifolia* over 1−3 years of growth based on the ultrahigh-performance liquid chromatography−quadrupole time-of-flight mass spectrometry (UHPLC−Q-TOF/MS) and proton nuclear magnetic resonance (^{1}H NMR) metabolomics methods. The results showed that the chemical constituents of *P. tenuifolia* grown for 1 year differed from those grown for 2 or 3 years.

In this study, the metabolites, 8 main active substances, and 12 trace elements of different years—1 (Y1), 3 (Y3), and 5 (Y5) years—of *O. caudatum* were determined, and the effects of the growth years on the quality of *O. caudatum* were objectively and comprehensively revealed. This study provides new ideas for the comprehensive evaluation of medicinal value and important theoretical support for the development of harvest times.

2. RESULTS

2.1. Active Substances in *O. caudatum* for Different Growth Years. The chemical constituents of *O. caudatum* are complex, and the main active substances include saponins, polysaccharides, flavonoids, terpenoids, and alkaloids. In this study, the contents of total saponins, total polysaccharides, total flavonoids, total polyphenols, total sterols, total triterpenoids, total alkaloids, and crude protein were determined (Figure 1A). The results showed that the total protein, polysaccharide, and saponin contents were the highest. The highest protein content was 9.24 ± 0.23%. The polysaccharide content of different years of *O. caudatum* was ≥5%, and the saponin content was ≥3%. The saponin and sterol contents increased with growth years, whereas the total polysaccharide content decreased. The total alkaloid, crude protein, and total triterpenoid contents initially decreased and then increased with age. The total polyphenol and flavonoid contents showed a negligible change with increasing years of growth. In summary, the main substances of *O. caudatum* changed significantly in different years of growth.

2.2. Elemental Contents of *O. caudatum* for Different Growth Years. An inductively coupled plasma mass spectrometry (ICP−MS) system was used to determine the trace element contents, including sodium (Na), potassium (K), magnesium (Mg), iron (Fe), zinc (Zn), calcium (Ca), manganese (Mn), arsenic (As), mercury (Hg), copper (Cu), lead (Pb), and cadmium (Cd). As shown in Figure 1B, the contents of Ca, K, and Mg were higher in *O. caudatum*, with the highest contents being 15.76 ± 1.73, 28.00 ± 1.60, and 2.03 ± 0.07 g/Kg, respectively. Cu and Zn contents increased with age, whereas the Fe content decreased. Na and K contents initially decreased and then increased with age. Ca, Mg, and Mn contents initially increased and then remained relatively stable. However, the contents of heavy metals such as As, Cd, Hg, and Pb did not change significantly with the growing years (Figure 1C).

2.3. Method Validation. To further study the changing trends of metabolites with growth years, UHPLC tandem mass spectrometry (UHPLC−MS/MS) was used to analyze the metabolic profiles of *O. caudatum*. First, the stability of the UHPLC−MS/MS system was evaluated by comparing the mass spectrum base peak map of the quality control (QC) samples and principal component analysis (PCA) statistical analysis of the overall sample. The base peaks of QC samples in the positive and negative ion detection modes were compared (Figure 2A). The results showed that the response intensities and retention times of each chromatographic peak were essentially the same, indicating that the variation caused by instrument error was small and the data quality was reliable.

https://doi.org/10.1021/acsomega.3c02310
ACS Omega 2023, 8, 23889−23900

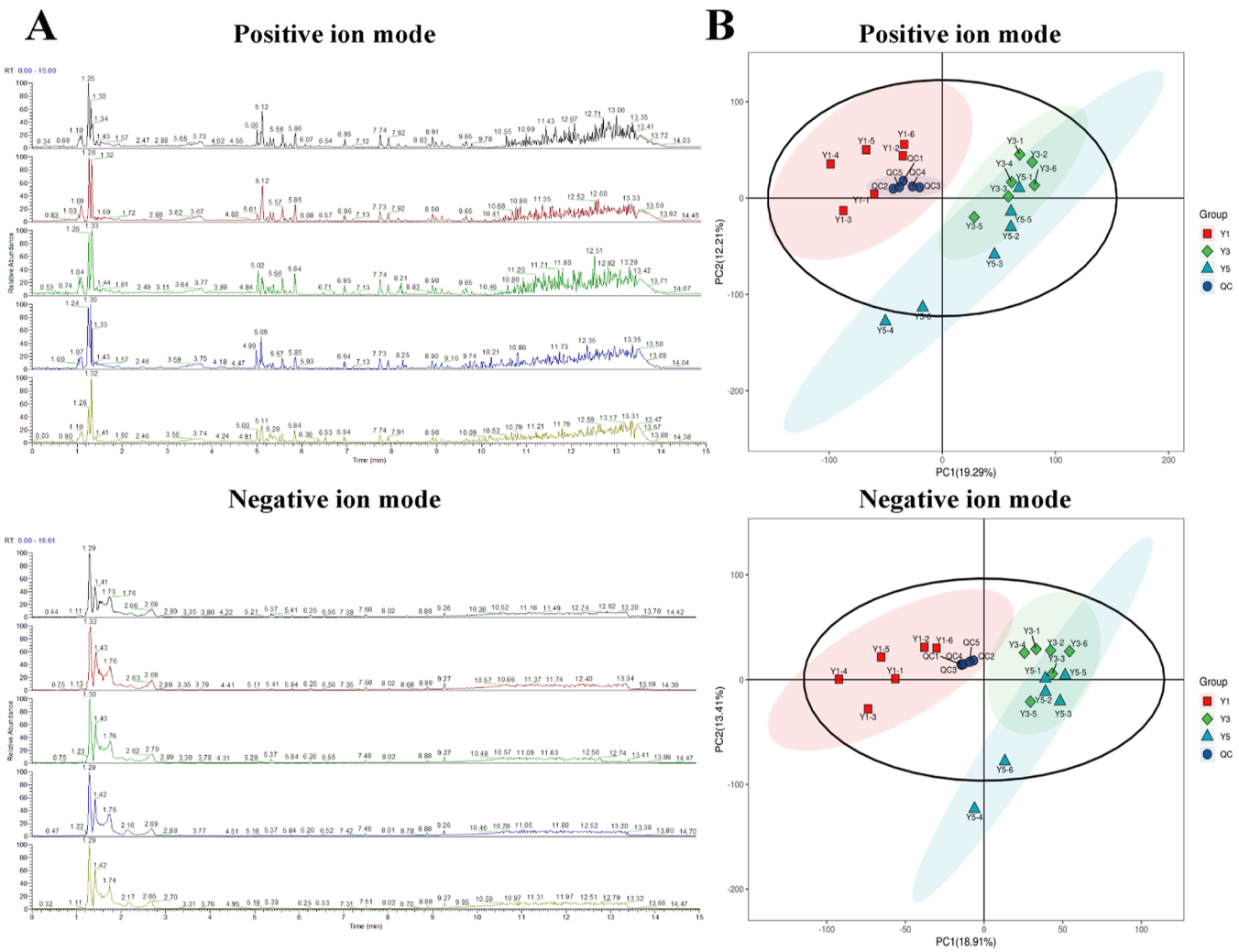

Figure 2. Mass spectrum base peak map comparison of QC samples and PCA statistical analysis of the overall sample. (A) Base peak spectra in positive and negative ion modes; (B) PCA score chart in positive and negative ion modes. QC: quality control samples; Y1: 1 year old *O. caudatum*; Y3: 3 year old *O. caudatum*; Y5: 5 year old *O. caudatum*.

The PCA model obtained by 7-fold cross-validation of all experimental and QC samples is shown in Figure 2B. The QC samples were closely clustered, indicating good repeatability of the experiment. In summary, the instrument analysis system used exhibited good stability, and the experimental data were stable and reliable.

2.4. Principal Component Analysis. A total of 1954 metabolites were identified among all samples (as shown in Supporting Information S1). PCA was performed to attain a global view of the metabolic profiles of all samples. As shown in Figure 3B, the spatial distances between samples Y3 and Y5 were relatively close. However, the Y1 samples differed slightly from the Y3 and Y5 samples on the PCA map. These results show that the metabolic differences between the Y3 and Y5 samples were small, and the metabolites of the Y1 samples differed from those of the other groups.

2.5. Orthogonal Partial Least Square Discriminant Analysis. To confirm the metabolic differences among *O. caudatum* samples from different growth years, orthogonal partial least square discriminant analysis (OPLS_DA) was used to optimize group separation (parameters shown in Table1). The pairwise comparison among the Y1, Y3, and Y5 samples revealed significant metabolic differences among the different group samples in each pairwise comparison of the first component (Figure 3A). OPLS_DA models with high R^2Y and Q^2 values were constructed, as shown in Table 1, and showed excellent fit and satisfactory predictive power. Furthermore, the OPLS_DA model was evaluated using permutation tests (Figure 3B) for possible overfitting. A 200-time permutation test was performed. The R^2 intercepts for samples Y1 and Y3 were 0.908, Y1 and Y5 were 0.925, and Y3 and Y5 were 0.994, and the Q^2 intercepts were −0.733, −0.813, and −0.377, respectively. The above results confirm that the OPLS_DA model was not overfitted and that the data generated by the model are credible.

2.6. Comparative Analysis of Differential Metabolites. The variable importance in projection (VIP) values obtained from the OPLS_DA model was used to identify different metabolites with biological significance. In this experiment, VIP > 1 was used as the threshold to preliminarily screen for differential metabolites among the three groups. One-way analysis of variance (ANOVA) was used to verify whether there was a significant difference in the metabolites. Among the three groups, 156 differential metabolites (as shown in Supporting Information S2) with VIP values greater than 1.0 and $p < 0.05$ were identified, including 18 amino

https://doi.org/10.1021/acsomega.3c02310
ACS Omega 2023, 8, 23889−23900

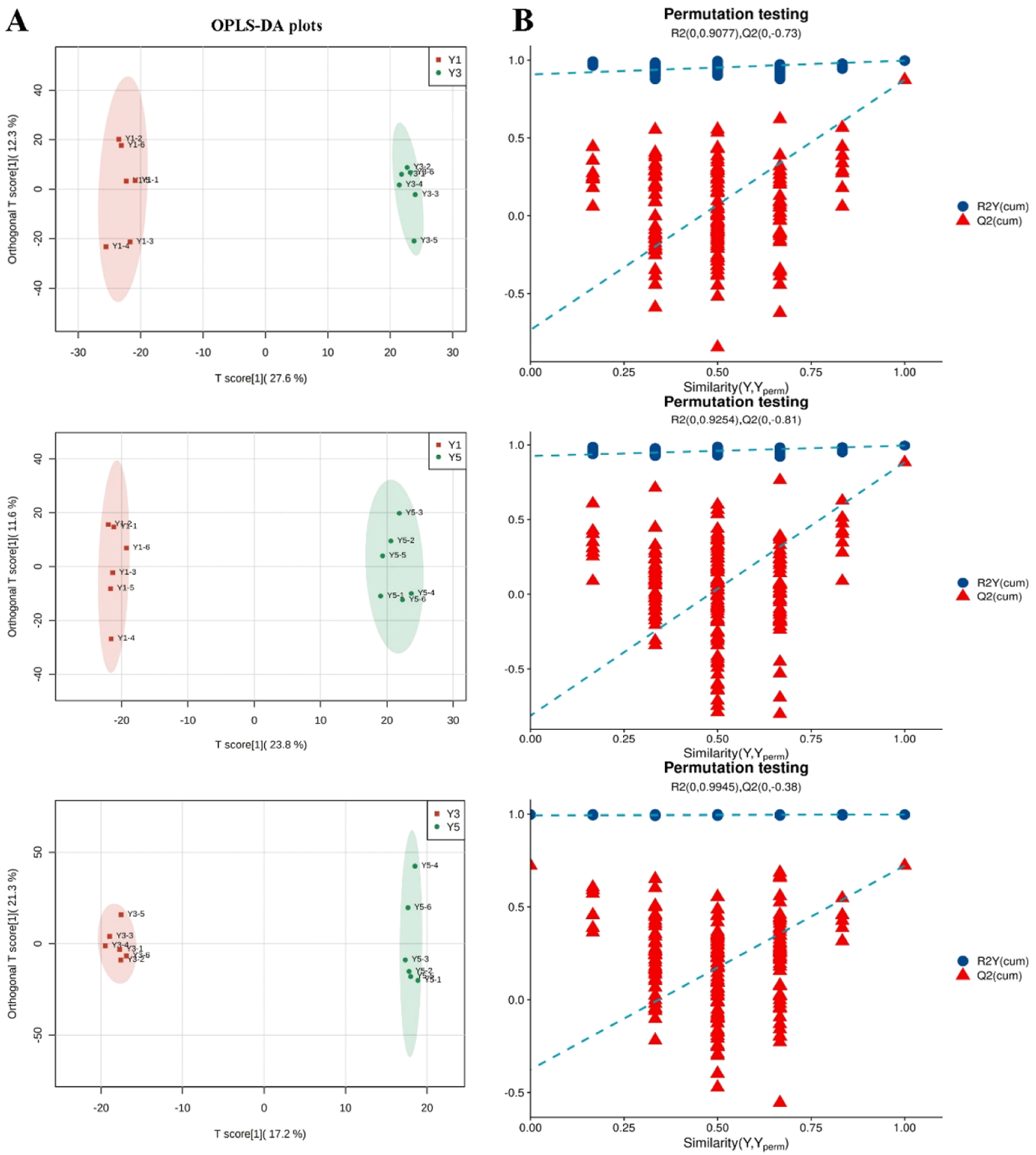

Figure 3. Scatter plots and permutation tests of the OPLS_DA model. (A) OPLS_DA analyses for Y1 vs Y3, Y1 vs Y5, and Y3 vs Y5; (B) permutation tests for Y1 vs Y3, Y1 vs Y5, and Y3 vs Y5. Y1: 1 year old *O. caudatum*; Y3: 3 year old *O. caudatum*; Y5: 5 year old *O. caudatum*.

Table 1. PCA and OPLS_DA Model Parameters

no	type	A	*N*	R^2X(cum)	R^2Y(cum)	Q^2(cum)	R^2 intercept	Q^2 intercept
all	PCA	4	18	0.548		0.588		
Y1/Y3	OPLS-DA	1 + 1 + 0	12	0.400	0.997	0.874	0.908	−0.733
Y1/Y5	OPLS-DA	1 + 1 + 0	12	0.354	0.996	0.884	0.925	−0.813
Y3/Y5	OPLS-DA	1 + 2 + 0	12	0.463	0.998	0.723	0.994	−0.377

https://doi.org/10.1021/acsomega.3c02310
ACS Omega 2023, 8, 23889−23900

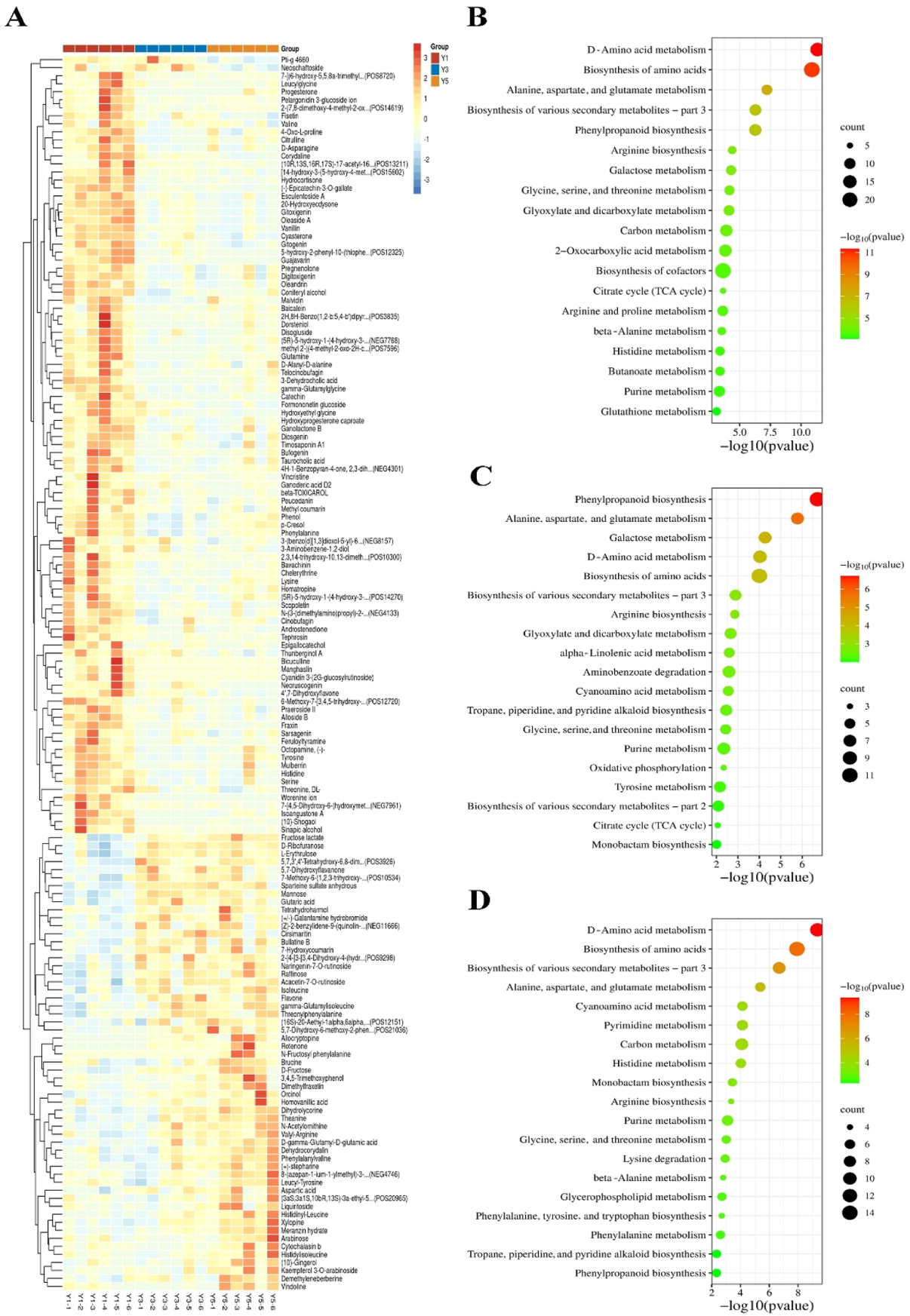

Figure 4. Expression profiling changes and KEGG enrichment bubble diagram of differential metabolites in *O. caudatum* for different growth years. (A) Heat map analysis; (B–D) KEGG analysis: (B) Y1 vs Y3, (C) Y1 vs Y5, and (D) Y3 vs Y5. Y1: 1 year old *O. caudatum*; Y3: 3 year old *O. caudatum*; Y5: 5 year old *O. caudatum*.

https://doi.org/10.1021/acsomega.3c02310
ACS Omega 2023, 8, 23889–23900

Table 2. Sugars, Amino Acid Metabolites, and Oligopeptides Identified in *O. caudatum*[a]

compound class	no	metabolites	molecular mass	RT [min]	*m/z*	fold change		
						Y1/Y3	Y1/Y5	Y3/Y5
amino acid	1	4-oxo-L-proline	130.05	1.26	130.05	2.70	1.77	0.66
	2	aspartic acid	134.04	1.24	134.04	0.73	0.61	0.83
	3	citrulline	176.10	1.31	176.10	9.54	2.63	0.28
	4	asparagine	131.04	1.22	131.05	2.58	1.96	0.76
	5	glutamine	147.08	1.55	147.08	1.76	1.42	0.80
	6	glutaric acid	115.04	1.32	115.04	1.04	0.58	0.56
	7	histidine	154.06	1.21	154.06	2.68	1.86	0.70
	8	hydroxyethyl glycine	118.05	1.27	118.05	2.27	3.84	1.69
	9	isoleucine	132.10	2.01	132.10	0.70	0.60	0.86
	10	lysine	164.14	8.94	164.14	0.53	0.73	1.37
	11	*N*-acetylornithine	173.09	2.82	173.09	3.10	2.54	0.82
	12	*N*-fructosyl phenylalanine	328.14	5.11	328.14	1.77	0.10	0.06
	13	phenylalanine	166.09	5.11	166.09	2.92	1.66	0.57
	14	serine	104.03	1.22	104.04	2.87	2.49	0.87
	15	theanine	175.11	2.80	175.11	2.59	1.14	0.44
	16	threonine	120.07	1.27	120.07	1.37	1.65	1.20
	17	tyrosine	182.08	3.89	182.08	2.77	1.53	0.55
	18	valine	118.09	2.20	118.09	1.97	2.17	1.10
oligopeptides	19	gamma-Glu−Gly	205.08	3.11	205.08	2.92	2.30	0.79
	20	Ala−Ala	161.09	1.39	161.09	1.80	1.39	0.77
	21	gamma-Gln−Glu	277.10	1.73	277.10	0.55	0.41	0.75
	22	gamma-Gln−Ile	259.13	5.02	259.13	0.54	0.52	0.95
	23	His−Leu	269.16	3.06	269.16	0.52	0.27	0.53
	24	His−Ile	267.15	3.14	267.15	1.15	0.53	0.47
	25	Leu−Gly	189.12	1.37	189.12	0.47	0.59	1.25
	26	Leu−Tyr	295.17	5.42	295.17	1.04	0.73	0.70
	27	Phe−Ala	265.15	5.36	265.15	0.69	0.50	0.72
	28	Tre−Phe	265.12	5.07	265.12	0.54	0.56	1.05
	29	Val−Arg	274.19	1.39	274.19	0.58	0.47	0.82
sugar	30	fructose lactate	267.07	1.31	267.07	0.66	0.47	0.72
	31	fructose	198.10	1.30	198.10	0.46	0.35	0.77
	32	ribofuranose	131.03	1.31	131.03	0.57	0.61	1.07
	33	raffinose	539.14	2.56	539.14	0.59	0.50	0.85
	34	erythrulose	119.03	1.30	119.03	0.64	0.66	1.04
	35	arabinose	149.04	5.29	149.05	1.18	0.63	0.54
	36	mannose	163.06	1.35	163.06	0.25	0.29	1.18

[a]Y1: 1 year old *O. caudatum*; Y3: 3 year old *O. caudatum*; Y5: 5 year old *O. caudatum*. Y1/Y3: ratio of Y1 to Y3; Y1/Y5: ratio of Y1 to Y5; Y3/Y5: ratio of Y3 to Y5.

acids, 11 oligopeptides, 7 sugars, 4 saponins, 29 flavonoids, 8 isoflavonoids, 16 phenols, 7 triterpenoids, 17 steroids, 20 alkaloids, and 19 coumarins. Heatmap analysis was performed to visualize the dynamic metabolite changes of *O. caudatum* in different growth years. As shown in Figure 4A, the levels of these metabolites in the Y3 and Y5 samples were significantly different from those in the Y1 sample. The upper part of Figure 4A shows significantly reduced metabolites in the Y3 and Y5 samples compared with those in the Y1 samples, including leucylglycine, neoschaftoside, fisetin, and phenol. The lower part of Figure 4A shows significantly increased metabolites in the Y3 and Y5 samples compared with that in the Y1 samples, including meranzin hydrate, xylopine, dihydrolycorine, and *N*-acetylornithine.

2.7. Amino Acids, Oligopeptides, and Sugars in Different Growth Years. Amino acids and oligopeptides are the main components of the body and have important biological activities.[19] This study identified 18 amino acids (5 essential and 13 nonessential amino acids) and 11 oligopeptides in *O. caudatum* from different growth years (Table 2). The contents of most amino acids decreased at first and then increased with age, which was consistent with the trend for total protein. The aspartic acid and isoleucine contents increased with age, whereas the hydroxyethyl glycine, threonine, and valine contents decreased. However, the contents of most oligopeptides increased with age. The contents of gamma_Glu_Gly, Ala_Ala, His_Ile, and Leu_Tyr first decreased and then increased with age, whereas the contents of Leu_Gly and Tre_Phe first increased and then decreased.

Polysaccharides are important active substances in plants and have many physiological functions, such as antidiabetic, antitumor, and immunity-enhancing effects.[20,21] The compositions and proportions of monosaccharides in polysaccharides significantly affect their activity.[22] As shown in Table 2, seven sugars were identified in this study. The fructose, lactate, fructose, and raffinose contents increased with age. The ribofuranose, erythrulose, and mannose contents initially increased and then decreased, whereas the arabinose content initially decreased and then increased. Considering the high

https://doi.org/10.1021/acsomega.3c02310
ACS Omega 2023, 8, 23889−23900

Table 3. Summary of Saponins, Flavonoids, Isoflavonoids, Phenols, Triterpenoids, Steroids, Alkaloids, and Coumarins Identified in *O. caudatum*[a]

compound class	no	metabolites	molecular mass	RT [min]	*m/z*	fold change Y1/Y3	Y1/Y5	Y3/Y5
saponins	1	furostane base −1H2O +1O, *O*-Hex, *O*-Hex−Hex	917.48	6.78	917.48	2.03	3.32	1.64
	2	esculentoside A	849.43	6.97	849.42	2.31	2.72	1.18
	3	medicagenic acid base + *O*-malonylHex	751.39	7.39	751.39	2.01	2.52	1.25
	4	spirostane −2H, +1O, *O*-Hex−Hex, $C_6H_9O_4$	943.46	7.73	943.45	3.90	2.58	0.66
	5	timosaponin A1	579.39	6.35	579.39	2.04	1.91	0.94
	6	disogluside	577.37	5.74	577.37	2.48	2.07	0.84
	7	alloside B	803.44	6.34	803.44	2.81	2.95	1.05
flavonoids	8	cyasterone	521.31	7.47	521.31	1.88	2.90	1.54
	9	(*Z*)-2-benzylidene-9-(quinolin-4-yl)-8,9-dihydro-2*H*-furo[2,3-*f*]chromene-3,7-dione	442.10	3.37	442.10	0.58	0.86	1.48
	10	(−)-epicatechin-3-*O*-gallate	441.15	13.40	441.15	4.85	5.36	1.11
	11	5-hydroxy-2-phenyl-10-(thiophen-3-yl)-9,10-dihydropyrano[2,3-*f*]chromene-4,8-dione	413.05	5.62	413.05	5.36	25.81	4.82
	12	guajavarin	433.08	1.30	433.08	14.77	39.11	2.65
	13	4′,7-dihydroxyflavone	255.07	5.24	255.07	1.81	7.23	3.99
	14	fisetin	285.13	6.75	285.13	1.88	3.46	1.84
	15	bavachinin	337.20	9.25	337.20	4.64	3.59	0.78
	16	5,7-dihydroxy-6-methoxy-2-phenylchromen-4-one	283.14	9.62	283.14	0.32	0.17	0.54
	17	acacetin-7-*O*-rutinoside	637.18	1.40	637.18	0.68	0.69	1.02
	18	catechin	291.08	5.06	291.09	68.72	17.30	0.25
	19	naringenin-7-*O*-rutinoside	579.18	2.56	579.17	0.70	0.88	1.25
	20	kaempferol 3-*O*-arabinoside	417.12	1.66	417.12	0.95	0.40	0.42
	21	manghaslin	755.20	5.27	755.20	122.15	97.29	0.80
	22	epigallocatechol	307.08	2.95	307.08	2.43	5.54	2.28
	23	4*H*-1-benzopyran-4-one, 2,3-dihydro-7-hydroxy-2-(4-hydroxyphenyl)-	255.12	7.26	255.12	3.66	2.07	0.57
	24	cyanidin 3-(2G-glucosylrutinoside)	757.22	5.27	757.22	257.64	119.86	0.47
	25	5,7,3′,4′-tetrahydroxy-6,8-dimethoxyflavone	345.10	1.32	345.10	0.25	0.27	1.07
	26	pelargonidin 3-glucoside ion	431.10	1.36	431.10	6.63	4.38	0.66
	27	7-[4,5-dihydroxy-6-(hydroxymethyl)-3-(3,4,5-trihydroxy-6-methyloxan-2-yl) oxyoxan-2-yl]oxy-5-hydroxy-2-(4-methoxyphenyl)-2,3-dihydrochromen-4-one	595.20	6.15	595.20	0.49	0.38	0.77
	28	liquiritoside	419.13	7.50	419.13	0.97	0.47	0.48
	29	2-[4-[3-[3,4-dihydroxy-4-(hydroxymethyl)oxolan-2-yl]oxy-4,5-dihydroxy-6-(hydroxymethyl)oxan-2-yl]oxyphenyl]-7-hydroxy-2,3-dihydrochromen-4-one	549.17	2.56	549.16	0.47	0.49	1.04
	30	flavone	221.07	13.82	221.06	0.40	0.48	1.22
	31	mulberrin	421.17	5.50	421.17	5.41	2.54	0.47
	32	baicalein	292.93	1.20	292.94	3.52	2.21	0.63
	33	neoschaftoside	563.23	5.40	563.23	0.79	3.54	4.49
	34	cirsimaritin	353.04	1.49	353.04	0.09	0.12	1.44
	35	5,7-dihydroxyflavanone	279.07	1.35	279.06	0.02	0.04	1.70
	36	cyasterone	521.31	7.47	521.31	1.88	2.90	1.54
isoflavonoids	37	formononetin glucoside	429.19	11.52	429.20	2.36	7.95	3.37
	38	beta-TOXICAROL	409.24	9.74	409.24	1.35	1.45	1.08
	39	isoangustone A	423.18	5.49	423.18	4.46	2.75	0.62
	40	3-(benzo[*d*][1,3]dioxol-5-yl)-6-ethyl-7-isopropoxy-2-methyl-4*H*-chromen-4-one	367.15	8.65	367.15	1.32	2.13	1.61
	41	tephrosin	409.13	8.97	409.13	4.27	5.62	1.32
	42	rotenone	395.20	5.00	395.20	0.14	0.04	0.27
	43	8-(azepan-1-ium-1-ylmethyl)-3-(2,4-dimethoxyphenyl)-2-oxo-2*H*-chromen-7-olate	410.19	5.46	410.20	1.04	0.56	0.54
	44	Pti-g 4660	271.06	7.44	271.06	0.92	2.30	2.49
phenols	45	vanillin	153.05	7.51	153.05	2.13	2.60	1.22
	46	(10)-shogaol	350.27	10.49	350.27	2.46	1.46	0.59
	47	orcinol	125.06	0.97	125.06	0.57	0.46	0.81
	48	coniferyl alcohol	163.07	1.32	163.08	2.60	1.95	0.75
	49	(5*R*)-5-hydroxy-1-(4-hydroxy-3-methoxyphenyl)tetradecan-3-one	349.24	7.72	349.24	3.40	1.03	0.30
	50	sinapic alcohol	211.10	5.73	211.10	2.97	3.25	1.10
	51	(10)-gingerol	373.23	5.57	373.23	1.39	2.29	1.65
	52	feruloyltyramine	312.12	6.84	312.12	8.91	7.13	0.80
	53	3-aminobenzene-1,2-diol	126.06	1.27	126.05	2.11	2.09	0.99
	54	3,4,5-trimethoxyphenol	185.08	13.73	185.08	0.80	0.28	0.35
	55	homovanillic acid	165.05	13.88	165.05	0.76	0.40	0.53
	56	*p*-cresol	91.05	5.10	91.05	2.22	1.40	0.63

https://doi.org/10.1021/acsomega.3c02310
ACS Omega 2023, 8, 23889−23900

Table 3. continued

compound class	no	metabolites	molecular mass	RT [min]	*m/z*	fold change Y1/Y3	fold change Y1/Y5	fold change Y3/Y5
	57	phenol	95.05	5.10	95.05	2.04	1.34	0.66
	58	octopamine, (−)-	136.08	3.43	136.08	2.60	1.51	0.58
	59	(5*R*)-5-hydroxy-1-(4-hydroxy-3-methoxyphenyl)tetradecan-3-one	349.24	8.65	349.24	3.40	1.03	0.30
	60	malvidin	331.00	2.83	331.00	19.50	2.12	0.11
triterpenoids	61	gitogenin	433.33	6.28	433.33	2.41	4.13	1.71
	62	esculentoside A	849.43	7.61	849.42	2.31	2.72	1.18
	63	diosgenin	415.32	5.74	415.32	1.61	1.97	1.22
	64	neoruscogenin	429.30	9.86	429.30	2.83	17.11	6.04
	65	ganoderic acid D2	553.28	9.34	553.28	3.17	5.50	1.74
	66	sarsagenin	399.33	6.46	399.33	1.88	2.17	1.15
	67	ganolactone B	459.27	6.89	459.27	2.99	2.27	0.76
steroids and derivatives	68	(10*R*,13*S*,16*R*,17*S*)-17-acetyl-16-ethyl-10,13-dimethyl-2,3,4,7,8,9,10,11,12,13,14,15,16,17-tetradecahydro-1*H*-cyclopenta[*a*]phenanthren-3-yl acetate	409.27	10.62	409.27	2.10	2.31	1.10
	69	20-hydroxyecdysone	503.30	7.47	503.30	2.19	3.12	1.43
	70	gitoxigenin	373.24	7.48	373.24	2.31	2.96	1.28
	71	hydrocortisone	363.25	6.26	363.25	3.75	0.53	0.14
	72	[14-hydroxy-3-(5-hydroxy-4-methoxy-6-methyloxan-2-yl)oxy-10,13-dimethyl-17-(5-oxo-2*H*-furan-3-yl)-1,2,3,4,5,6,7,8,9,11,12,15,16,17-tetradecahydrocyclopenta[*a*]phenanthren-16-yl] acetate	599.32	7.47	599.32	2.20	2.75	1.25
	73	androstenedione	287.20	6.94	287.20	2.49	3.28	1.31
	74	oleandrin	577.34	7.39	577.34	2.11	2.13	1.01
	75	hydroxyprogesterone caproate	429.30	8.59	429.30	4.98	3.77	0.76
	76	2,3,14-trihydroxy-10,13-dimethyl-17-(2,3,6,7-tetrahydroxy-6-methylheptan-2-yl)-2,3,4,5,9,11,12,15,16,17-decahydro-1*H*-cyclopenta[*a*]phenanthren-6-one	497.31	9.34	497.31	2.86	3.70	1.30
	77	pregnenolone	339.23	7.28	339.23	2.26	1.82	0.81
	78	digitoxigenin	375.25	7.28	375.25	2.56	1.85	0.72
	79	3-dehydrocholic acid	405.26	6.02	405.26	36.61	3.29	0.09
	80	cinobufagin	443.24	7.17	443.24	2.04	1.92	0.94
	81	taurocholic acid	516.30	5.52	516.30	5.89	2.39	0.41
	82	bufogenin	407.22	9.59	407.22	8.09	3.79	0.47
	83	telocinobufagin	425.23	8.71	425.23	5.87	2.89	0.49
	84	progesterone	315.23	5.95	315.23	21.86	3.15	0.14
alkaloids and derivatives	85	worenine ion	335.11	5.17	335.11	44.91	86.71	1.93
	86	corydaline	368.18	5.08	368.19	2.56	0.77	0.30
	87	sparteine sulfate anhydrous	330.91	1.06	330.91	0.15	0.16	1.12
	88	(16*S*)-20-aethyl-1alpha,6alpha,16-trimethoxy-4-methoxymethyl-aconitan-8,14alpha-diol	474.28	9.25	474.28	0.54	0.41	0.75
	89	dehydrocorydalin	366.17	5.36	366.17	0.87	0.56	0.65
	90	demethyleneberberine	347.11	5.75	347.11	0.59	0.40	0.67
	91	vincristine	462.19	5.29	462.19	4.52	6.23	1.38
	92	tetrahydroharmol	203.12	7.89	203.12	0.65	0.54	0.83
	93	bullatine B	460.27	8.91	460.27	0.57	0.62	1.08
	94	(3*aS*,3*a*1*S*,10*bR*,13*S*)-3*a*-ethyl-5-(methoxycarbonyl)-1,2,3,3*a*,3*a*1,4,6,11,12,13-decahydroindolizino[8,1-*cd*]carbazol-13-ium iodide	362.19	5.07	362.19	1.03	0.63	0.62
	95	(+/−)-galantamine hydrobromide	368.08	2.60	368.08	0.45	0.47	1.04
	96	homatropine	276.16	5.82	276.16	18.91	2.35	0.12
	97	vindoline	439.22	5.99	439.22	5.03	0.36	0.07
	98	dihydrolycorine	290.13	2.45	290.14	0.45	0.31	0.69
	99	allocryptopine	370.16	1.38	370.16	0.12	0.04	0.37
	100	brucine	394.19	9.78	394.19	1.03	0.69	0.67
	101	xylopine	296.12	3.01	296.13	0.68	0.47	0.70
	102	(+)-stepharine	320.12	5.50	320.13	0.88	0.58	0.66
	103	bicuculline	406.07	5.26	406.07	136.40	246.08	1.81
	104	cytochalasin b	502.26	7.39	502.26	2.91	0.25	0.08
coumarins and derivatives	105	fraxin	369.08	6.19	369.08	8.27	12.03	1.45
	106	6-methoxy-7-[3,4,5-trihydroxy-6-(hydroxymethyl)oxan-2-yl]oxychromen-2-one	399.09	5.75	399.09	2.67	6.53	2.45
	107	chelerythrine	349.13	9.25	349.13	3.32	2.74	0.83
	108	oleaside A	539.30	7.47	539.30	2.40	3.15	1.31
	109	meranzin hydrate	320.14	2.19	320.15	24.97	3.36	0.13
	110	thunberginol A	271.06	6.54	271.06	1.43	2.17	1.52

https://doi.org/10.1021/acsomega.3c02310
ACS Omega 2023, 8, 23889−23900

Table 3. continued

compound class	no	metabolites	molecular mass	RT [min]	m/z	fold change Y1/Y3	Y1/Y5	Y3/Y5
	111	scopoletin	210.08	5.06	210.08	0.18	0.09	0.48
	112	praeroside II	469.13	6.17	469.14	2.01	2.80	1.39
	113	peucedanin	276.13	5.25	276.12	2.27	2.44	1.07
	114	methyl 2-((4-methyl-2-oxo-2*H*-chromen-7-yl)oxy)propanoate	263.09	2.36	263.09	19.03	6.08	0.32
	115	methyl coumarin	161.06	5.52	161.06	2.00	2.20	1.10
	116	dimethylfraxetin	237.08	13.73	237.08	0.67	0.29	0.43
	117	2-(7,8-dimethoxy-4-methyl-2-oxo-2*H*-chromen-3-yl)-*N*-(1-isopropyl-1*H*-indol-4-yl)acetamide	435.19	6.00	435.19	37.34	14.20	0.38
	118	7-[(6-hydroxy-5,5,8a-trimethyl-2-methylidene-decahydronaphthalen-1-yl) methoxy]-2*H*-chromen-2-one	421.17	5.50	421.18	21.66	11.49	0.53
	119	*N*-(3-(dimethylamino)propyl)-2-((3,4,8,8-tetramethyl-2-oxo-2,8,9,10-tetrahydropyrano[2,3-*f*]chromen-5-yl)oxy)acetamide	417.23	5.12	417.24	2.12	1.70	0.81
	120	2*H*,8*H*-benzo(1,2-*b*:5,4-*b*′)dipyran-2-one, 10-methoxy-8,8-dimethyl-	259.09	2.43	259.10	143.65	7.17	0.05
	121	dorsteniol	261.07	2.36	261.08	40.45	4.75	0.12
	122	7-hydroxycoumarin	163.04	7.70	163.04	0.70	0.75	1.08
	123	7-methoxy-6-(1,2,3-trihydroxy-3-methylbutyl)chromen-2-one	295.12	8.91	295.12	0.74	0.80	1.09

[a]Y1: 1 year old *O. caudatum*; Y3: 3 year old *O. caudatum*; Y5: 5 year old *O. caudatum*. Y1/Y3: ratio of Y1 to Y3; Y1/Y5: ratio of Y1 to Y5; Y3/Y5: ratio of Y3 to Y5.

protein and polysaccharide contents in *O. caudatum*, the changing trends in amino acids and sugars require further study.

2.8. Saponins, Flavonoids, Isoflavonoids, Phenols, Triterpenoids, Steroids, Alkaloids, and Coumarins in Different Growth Years. The levels of most saponins, flavonoids, isoflavonoids, triterpenoids, and coumarins decreased with age (Table 3). Most phenols and steroids initially decreased and then increased with age. The abundance of most alkaloids and their derivatives increased during the entire study period. These changes directly affected the quality of *O. caudatum* during the different growth periods. Detailed information is provided in Table 2. Among the three groups, a total of 16 metabolites were obtained, showing an increasing trend with age, including 5,7-dihydroxy-6-methoxy-2-phenylchromen-4-one, kaempferol 3-*O*-arabinoside, 7-[4,5-dihydroxy-6-(hydroxymethyl)-3-(3,4,5-trihydroxy-6-methyloxan-2-yl)-oxyoxan-2-yl]oxy-5-hydroxy-2-(4-methoxyphenyl)-2,3-dihydrochromen-4-one, liquiritoside, rotenone, orcinol, 3,4,5-trimethoxyphenol, homovanillic acid, (16*S*)-20-aethyl-1alpha,6alpha,16-trimethoxy-4-methoxymethyl-aconitan-8,14alpha-diol, dehydrocorydalin, demethyleneberberine, tetrahydroharmol, dihydrolycorine, allocryptopine, xylopine, (+)-stepharine, scopoletin, and dimethylfraxetin. These metabolites are of great significance in the search for age-identified markers for *O. caudatum*.

2.9. Metabolic Pathway Analysis. The differential metabolite data were subjected to Kyoto Encyclopedia of Genes and Genomes (KEGG) pathway analysis to understand the differences in the metabolic networks among the three groups of samples. Enriched pathways between the Y1 and Y3, Y1 and Y5, and Y3 and Y5 samples are shown in Figure 4B. The top ten pathways for the differentially expressed metabolites were identified, including D-amino acid metabolism; biosynthesis of amino acids; alanine, aspartate, and glutamate metabolism; biosynthesis of various secondary metabolites; phenylpropanoid biosynthesis; arginine biosynthesis; and glycine, serine, and threonine metabolism.

3. DISCUSSION

In traditional medicine, *O. caudatum* has significant effects on the treatment of hepatitis and liver cancer and antioxidation.[23] However, because it is not included in the pharmacopeia, the quality evaluation criteria are insufficient. Moreover, as a perennial plant, its medicinal ingredients change with age. The present study detected the main active substances of the different years of *O. caudatum* growth. The results showed that the content of active substances changed significantly with age. Saponins and sterols increased with age. In contrast, the polysaccharide content decreased with increasing age. Currently, saponins and polysaccharides are the main index substances in local standards. However, as the polysaccharides showed a decreasing trend with age, the use of polysaccharides as index substances requires further study.

To further study the changing trend of metabolites with growth years, UHPLC−MS/MS was used to study the metabolic spectrum. Based on PCA, metabolites of the 3 year old *O. caudatum* were similar to those of the 5 year old *O. caudatum* but differed from those of the 1 year old *O. caudatum*. Among the three groups, 156 differential metabolites with VIP values >1.0 and $p < 0.05$ were identified, including 18 amino acids, 11 oligopeptides, 7 sugars, 4 saponins, 29 flavonoids, 8 isoflavonoids, 16 phenols, 7 triterpenoids, 17 steroids, 20 alkaloids, and 19 coumarins.

To further understand multiple activities during metabolite accumulation, KEGG pathway enrichment analysis was carried out. The metabolic pathway was mainly enriched in the synthesis and metabolism of amino acids and the synthesis of secondary metabolites. Amino acids are the most basic substances that constitute biological proteins and are involved in many biological activities.[24] They are the basic units that constitute protein molecules in organisms and are closely related to biological activities. Furthermore, they have special physiological functions, such as producing antibodies, and are indispensable nutrients for organisms. Simultaneously, amino acids are important indicators for evaluating the nutritional value of food.[25] With an increase in growth years, the contents of most amino acids decreased at first and then increased, which is consistent with the trend of total protein. The aspartic

https://doi.org/10.1021/acsomega.3c02310
ACS Omega 2023, 8, 23889−23900

acid and isoleucine contents also increased with age. Aspartic acid can provide nitrogen sources for plants; however, asparagine can also be produced under the catalysis of aspartate transferase, which can be further converted into phenolic amide alkaloids.[26] With an increase in growth years, the isoleucine contents gradually increased; the accumulation of isoleucine plays an important role in plant adaptation to salt stress,[27] which is conducive to reducing salt stress damage to plants. The synthesis and metabolism of amino acids and proteins need to be further studied in the future.

O. caudatum saponins are the main active substances in *O. caudatum* and have antitumor and hepatoprotective effects.[28] In this study, relatively few saponins were detected, which may be related to their low degree of ionization. Various coumarins have been identified in *O. caudatum*, such as fraxin, chelerythrine, oleaside A, and meranzin hydrate. Presently, there are few studies on the pharmacological effects of coumarin in *O. caudatum*, which therefore deserve further attention. Saponins, flavonoids, sterols, and other active ingredients of *O. caudatum* exert different pharmacological effects. Therefore, clarifying the synthesis and accumulation of metabolites is of great significance for the rational utilization of *O. caudatum* resources.

In this study, 12 elements in *O. caudatum* were analyzed. The results showed higher K, Ca, and Mg contents. Ca, Mg, Fe, and Zn have good inhibitory effects on tumor cells. Zn and Cu in *O. caudatum* increased with the years of growth, but Zn/Cu was unchanged, <0.1%, which is consistent with previous studies.[29] Heavy metal ions such as As, Pb, and Hg can accumulate in the human body, affecting human health. Studies have shown that heavy metal ions in *O. caudatum* do not increase over time.

4. CONCLUSIONS

In this study, the contents of eight principal active substances in *O. caudatum* were studied; the results show that saponins and sterols increase with age. However, the polysaccharide content decreases. To further study metabolism profiling, UHPLC_MS/MS was performed. Among the three groups, 156 differential metabolites with VIP values greater than 1.0 and $p < 0.05$ were identified. Among the differential metabolites, 16 increased with increasing years of growth and have the potential to become age-identified markers. Finally, the trace element contents were studied; K, Ca, and Mg were high, and the ratio of Zn/Cu was less than 0.1%. Heavy metal ions in *O. caudatum* did not increase over time. The results of this study provide a basis to evaluate the edible values of *O. caudatum* and facilitate further exploitation. However, the study has a number of limitations. First, the number of samples was relatively small and should be increased in future work. UHPLC−MS/MS cannot detect all metabolites owing to the degree of metabolite ionization. Therefore, NMR is needed to further compensate for the shortcomings of UHPLC−MS/MS.

5. MATERIALS AND METHODS

5.1. Materials. All chemicals used in this study were of chromatographic grade for liquid chromatography (LC). Acetonitrile (ACN) (1.00030.4008), methanol (1.06007.4008), formic acid (FA) (111670), and ammonia (105426) were purchased from Merck (Darmstadt, Germany). *O. caudatum* plants were cultivated in the greenhouse of Changchun University of Chinese Medicine (Changchun, Jilin, China). The plant material (*O. caudatum* bulbs of Y1, Y3, and Y5 plants) for this study was collected in September 2022. The collected samples were identified by Dr. Hui-wei Bao (Changchun University of Chinese Medicine, Changchun, Jilin, China).

5.2. Main Active Substance Analysis in *O. caudatum* with Different Growth Years. The total saponins, polysaccharides, flavonoids, polyphenols, sterols, triterpenoids, alkaloids, and crude proteins of *O. caudatum* from different years of growth were analyzed in this study. Total saponins were extracted and evaluated using the vanillin−sulfuric acid method, total polysaccharides were evaluated using the phenol-sulfuric acid method, total flavonoids were evaluated using the aluminum nitrate colorimetric method, total polyphenols were evaluated using the Folin−Ciocalteu colorimetric method, and total triterpenoids were evaluated using the vanillin−perchloric acid method according to T/AHFIA 004-2018, SN/T 4260-2015, SN/T 4592-2016, T/AHFIA 005-2018, and NY/T 3676-2020, respectively. In addition, total sterols were evaluated using the sulfate−phosphate−ferric method following a previous study,[30] and total alkaloids were evaluated using the acid dye colorimetry method following a previous study.[31] Crude protein was analyzed using a BCA kit according to the manufacturer's instructions (Pierce, Rockford, IL, USA).

5.3. Analysis of Trace Element Contents. Dry bulbs of *O. caudatum* were digested by microwave digestion (ETHOS 1, MILESTONE, Shanghai, China). Nitric acid (5 mL) was added to 0.2 g of the sample, and the procedure was set as follows: 100 °C, 3 min; 140 °C, 3 min; 160 °C, 3 min; 180 °C, 3 min; and 190 °C, 15 min. When the temperature was below 50 °C, the digestion tank was removed, rinsed with ultrapure water, and diluted to 50 mL. ICP−MS equipment (iCAPQ, Thermo Scientific, San Jose, CA, USA) was used for elemental content analysis. The parameters were as follows: RF power, 1550 W; pump speed, 40 rpm; S/C temperature, 2.7 °C; sample depth, 5 mm; cool flow, 14 L/min; auxilliary flow, 0.8 L/min; and nebulizer flow, 1.122 L/min.

5.4. Metabolite Extraction. Six replicate samples for each growth year (1, 3, and 5 years) were sampled at the same position using a puncher (sampling position: middle part). The samples (80 mg) were ground in liquid nitrogen. Metabolites were extracted using 1 mL of a precooled mixture of methanol, ACN, and water (v/v/v, 2:2:1) and then subjected to ultrasonic shaking for 1 h in an ice bath. Subsequently, the mixture was placed at −20 °C for 1 h and centrifuged at 16,000×*g* for 20 min at 4 °C. The supernatant was recovered and concentrated to dryness under vacuum. During MS detection, 150 μL of methanol−water solution (1:1, v/v) was added to dissolve and centrifuged at 20,000×*g* for 20 min at 4 °C. Finally, the supernatant was used for MS analysis.

Additionally, to ensure data quality for metabolic profiling, QC samples were prepared by pooling aliquots of all samples that were representative of all samples under analysis and used for data normalization. The QC samples were prepared and analyzed using the same procedure as that used for the experimental samples in each batch.

5.5. UHPLC−MS/MS Analysis. Metabolomic profiling was performed using a UPLC-ESI-Q-Orbitrap-MS system (UHPLC, Shimadzu Nexera X2 LC-30AD, Shimadzu, Japan) coupled with Q-Exactive Plus (Thermo Scientific, San Jose, USA).

https://doi.org/10.1021/acsomega.3c02310
ACS Omega 2023, 8, 23889−23900

For LC separation, the samples were placed in a 4 °C automatic sampler and analyzed using an ACQUITY UPLC HSS T3 column (2.1 × 100 mm, 1.8 μm) (Waters, Milford, MA, USA). The injection volume was 6 μL, the column temperature was 40 °C, and the flow rate was 0.3 mL/min. The mobile phase contained buffer A: 0.1% FA in water and buffer B: ACN. Therefore, the gradient was set as follows: 0% buffer B, 2 min; 0−48% buffer B, 4 min; 48−100% buffer B, 4 min; 100% buffer B, 2 min; 100−0% buffer B, 0.1 min; and 0% buffer B, 2.9 min.

Electrospray ionization (ESI) in positive and negative modes was separately applied for MS data acquisition. The HESI source conditions were set as follows: spray voltage, 3.8 kV (positive) and 3.2 kV (negative); capillary temperature, 320 °C; sheath gas (nitrogen) flow, 30 arb (arbitrary units); aux gas flow, 5 arb; probe heater temp, 350 °C; and S-Lens RF level, 50. The instrument was set to acquire over the m/z range of 70−1050 Da for full MS. Full MS scans were acquired at a resolution of 70,000 at m/z 200 and 17,500 at m/z 200. The maximum injection time was set at 100 ms for MS and 50 ms for MS/MS. The isolation window for MS2 was set to 2 m/z, and the normalized collision energy (stepped) was set to 20, 30, and 40 for fragmentation.

5.6. Data Preprocessing and Filtering. Mass spectrometry data-independent analysis software 3.3 (MS-DIAL 3.3) was used to perform peak alignment, retention time correction, and peak area extraction. The metabolites were identified using accurate mass (mass tolerance < 10 ppm) and MS/MS (mass tolerance < 0.02 Da) data, which were matched with HMDB, MassBank, and other public databases. In the extracted-ion features, only the variables with more than 50% of the nonzero measurement values in at least one group were retained.

5.7. Metabonomic Data Analysis. R version 4.0.3 and R packages were used for all multivariate data analyses and modeling. Data were mean-centered using Pareto scaling. Models were built using PCA, orthogonal partial least squares discriminant analysis (OPLS_DA), and partial least squares discriminant analysis (PLS_DA). All evaluated models were tested for overfitting using permutation tests. The discriminating metabolites were identified using a statistically significant threshold of VIP values obtained from the OPLS_DA model and a two-tailed Student's t-test (p-value) on the normalized raw data at the univariate analysis level. The p-value was calculated using a one-way analysis of variance (ANOVA) for multiple-group analysis. Metabolites with VIP > 1.0 and p < 0.05 were considered statistically significant. To identify perturbed biological pathways, differential metabolite data were subjected to KEGG pathway analysis (http://www.kegg.jp). KEGG enrichment analyses were performed using Fisher's exact test, and FDR correction for multiple testing was performed. Enriched KEGG pathways were nominally statistically significant at p < 0.05.

■ ASSOCIATED CONTENT

Supporting Information

The Supporting Information is available free of charge at https://pubs.acs.org/doi/10.1021/acsomega.3c02310.

Total metabolites of UHPLC−MS/MS and differential metabolites among three groups (XLSX)

■ AUTHOR INFORMATION

Corresponding Author

Yang Xu − *Key Laboratory for Metabolic Regulation and Activity Research of Medicinal Plants, Baicheng Medical College, Baicheng, Jilin 137000, China; College of Life Sciences, Baicheng Normal University, Baicheng, Jilin 137000, China*; Email: 251748191@qq.com

Authors

Xueliang Zhao − *Key Laboratory for Metabolic Regulation and Activity Research of Medicinal Plants, Baicheng Medical College, Baicheng, Jilin 137000, China; College of Life Sciences, Baicheng Normal University, Baicheng, Jilin 137000, China*; orcid.org/0000-0003-2883-5133

Guangyu Lin − *Animal Husbandry Information Center, Changchun, Jilin 130000, China; Jilin Agricultural University, Changchun, Jilin 130018, China*

Tong Liu − *Key Laboratory for Metabolic Regulation and Activity Research of Medicinal Plants, Baicheng Medical College, Baicheng, Jilin 137000, China; College of Life Sciences, Baicheng Normal University, Baicheng, Jilin 137000, China*

Xue Zhang − *Key Laboratory for Metabolic Regulation and Activity Research of Medicinal Plants, Baicheng Medical College, Baicheng, Jilin 137000, China; College of Life Sciences, Baicheng Normal University, Baicheng, Jilin 137000, China*

Complete contact information is available at: https://pubs.acs.org/10.1021/acsomega.3c02310

Author Contributions

Xueliang Zhao and Yang Xu participated in the design, conducted the majority of the experiments, and drafted the manuscript. Tong Liu, Guangyu Lin, and Xue Zhang contributed to the interpretation of the findings and revised the manuscript. All authors read and approved the final manuscript.

Notes

The authors declare no competing financial interest.

■ ACKNOWLEDGMENTS

The authors thank Dr. Huiwei Bao for providing samples and Editage (www.editage.cn) for English language editing. The study was supported by the Program of Jilin Provincial Administration of Traditional Chinese Medicine (2023165 and 2022183).

■ REFERENCES

(1) Liu, D. Y.; Wang, K. Y.; Hang, Z. H.; Chen, W. H.; Chen, Z. L. Studies on the chemical constituents from Ognithogaum Caudatum Ait (I). *Chin. Tradit. Herb. Drugs* **1998**, *29*, 442−443.

(2) Chen, R. Z.; Li, Y.; Dong, H.; Liu, Z.; Li, S.; Yang, S.; Li, X. Optimization of ultrasonic extraction process of polysaccharides from Ornithogalum caudatum Ait and evaluation of its biological activities. *Ultrason. Sonochem.* **2012**, *19*, 1160−1168.

(3) Xiang, Z. O. U.; Zhou, L.; Zhang, Y.; Gong, T.; Ji, C. F.; Qu, Z. Y.; Liu, X.; Li, W. L. Study on the apoptotic mechanisms of human breast cancer MCF-7 cells induced by total saponins of Ornithogalum caudatum Ait. *Nat. Prod. Res. Dev.* **2020**, *32*, 32.

(4) Yu, Y. H.; Gao, L.; Shi, J.; Wang, L. P.; Sun, J. M.; Xu, Y. R.; Bai, B. Antitumor, analgesic, and anti-inflammatory effects of Ornithogalum caudatum extract. *Chin. Tradit. Herb. Drugs* **2013**, *44*, 2282−2284.

(5) Qu, Z. Y.; Shi, X.; Zou, X.; Yu, B. Study on the Apoptotic Mechanisms of Human Liver Cancer HepG-2 Cells Induced by Total Saponins of Ornithogalum caudatum. *J. Chin. Med. Mater.* **2016**, *39*, 867−871.
(6) Yuan, S.; Yin, S.; Liu, M.; Kong, J. Q. Isolation and characterization of a multifunctional flavonoid glycosyltransferase from Ornithogalum caudatum with glycosidase activity. *Sci. Rep.* **2018**, *8*, 5886.
(7) Chen, R.; Meng, F.; Liu, Z.; Chen, R.; Zhang, M. Antitumor activities of different fractions of polysaccharide purified from Ornithogalum caudatum Ait. *Carbohydr. Polym.* **2010**, *80*, 845−851.
(8) Yin, S.; Kong, J. Q. Transcriptome-guided discovery and functional characterization of two UDP-sugar 4-epimerase families involved in the biosynthesis of anti-tumor polysaccharides in Ornithogalum caudatum. *RSC Adv.* **2016**, *6*, 37370−37384.
(9) Tsugkiev, B. G.; Ramonova, E. V.; Kabisov, R. G. Antibiotic properties of Indian onion (Ornithogalum caudatum) against pathogenic and opportunistic-pathogenic microflora. *Proceedings of Gorsky State Agrarian University* **2015**, *3*, 225−228.
(10) Zhang, X.; Liu, X.; Zhang, Y.; Yang, A. H.; Zhang, Y. F.; Tong, Z. J.; Wang, Y. W. QiuWan-Nian-Qing, a Herbal Composite Prescription, Suppresses the Progression of Liver Cancer in Mice by Regulating Immune Response. *Front. Oncol.* **2021**, *11*, 696282.
(11) Pant, P.; Pandey, S.; Dall'Acqua, S. The influence of environmental conditions on secondary metabolites in medicinal plants: A literature review. *Chem. Biodiversity* **2021**, *18*, No. e2100345.
(12) Erb, M.; Kliebenstein, D. J. Plant secondary metabolites as defenses, regulators, and primary metabolites: the blurred functional trichotomy. *Plant Physiol.* **2020**, *184*, 39−52.
(13) Nicholson, J. K.; Lindon, J. C. Metabonomics. *Nature* **2008**, *455*, 1054−1056.
(14) Dong, X.; Yang, Z.; Wang, X.; Liu, Z.; Yu, H.; Peng, C.; Hou, X.; Lu, W.; Xing, Q.; Hu, J.; Huang, X.; Bao, Z.; Bao, Z. Metabonomic Analysis Provides New Insights into the Response of Zhikong Scallop (Chlamys farreri) to Heat Stress by Improving Energy Metabolism and Antioxidant Capacity. *Antioxidants* **2022**, *11*, 1084.
(15) Li, Z.; Bao, H. Anti-tumor effect of Inonotus hispidus petroleum ether extract in H22 tumor-bearing mice and analysis its mechanism by untargeted metabonomic. *J. Ethnopharmacol.* **2022**, *285*, 114898.
(16) Li, Z.; Bao, H. Comparative Analysis of Metabolic Compositions and Trace Elements of Inonotus hispidus Mushroom Grown on Five Different Tree Species. *ACS Omega* **2022**, *7*, 9343−9358.
(17) Li, Z.; Bao, H.; Han, C.; Song, M. The regular pattern of metabolite changes in mushroom Inonotus hispidus in different growth periods and exploration of their indicator compounds. *Sci. Rep.* **2022**, *12*, 14354.
(18) Xue, Y.; Li, X. W.; Li, Z. Y.; Zeng, F. S.; Zhang, F. S.; Li, A. P.; Qin, X. M.; Peng, B. UPLC/Q-TOF MS and NMR plant metabolomics approach in studying the effect of growth year on the quality of Polygala tenuifolia. *Acta Pharm. Sin. B* **2015**, *50*, 340−347.
(19) Proenza, A. M.; Oliver, J.; Palou, A.; Roca, P. Breast and lung cancer are associated with a decrease in blood cell amino acid content. *J. Nutr. Biochem.* **2003**, *14*, 133−138.
(20) Zhou, W.; Yang, T.; Xu, W.; Huang, Y.; Ran, L.; Yan, Y.; Mi, J.; Lu, L.; Sun, Y.; Zeng, X.; et al. The polysaccharides from the fruits of Lycium barbarum L. confer anti-diabetic effect by regulating gut microbiota and intestinal barrier. *Carbohydr. Polym.* **2022**, *291*, 119626.
(21) Fu, Y.; Wang, L.; Jiang, G.; Ren, L.; Wang, L.; Liu, X. Anti-Diabetic Activity of Polysaccharides from Auricularia cornea var. Li. *Foods* **2022**, *11*, 1464.
(22) Wang, H.; Li, H.; Hou, Y.; Zhang, P.; Tan, M. Plant polysaccharides: sources, structures, and anti-diabetic effects. *Curr. Opin. Food Sci.* **2023**, *51*, 101013.
(23) Zhang, Y.; Fang, F.; Fan, K.; Zhang, Y.; Zhang, J.; Guo, H.; Yu, P.; Ma, J. Effective cytotoxic activity of OSW-1 on colon cancer by inducing apoptosis in vitro and in vivo. *Oncol. Rep.* **2017**, *37*, 3509−3519.
(24) Chu, X. M.; Wang, C.; Liu, W.; Liang, L.; Gong, K.; Zhao, C.; Sun, K. Quinoline and quinolone dimers and their biological activities: An overview. *Eur. J. Med. Chem.* **2019**, *161*, 101−117.
(25) Day, L.; Cakebread, J.; Loveday, S. Food proteins from animals and plants: Differences in the nutritional and functional properties. *Trends Food Sci. Technol.* **2022**, *119*, 428−442.
(26) Kaya, C.; Ugurlar, F.; Farooq, S.; Ashraf, M.; Alyemeni, M. N.; Ahmad, P. Combined application of asparagine and thiourea improves tolerance to lead stress in wheat by modulating AsA-GSH cycle, lead detoxification and nitrogen metabolism. *Plant Physiol. Biochem.* **2022**, *190*, 119−132.
(27) Duan, M.; Yan, R. P.; Wang, Q. J.; Zhou, B. B.; Zhu, H. Y.; Liu, G. H.; Guo, X.; Zhang, Z. S. Integrated microbiological and metabolomics analyses to understand the mechanism that allows modified biochar to affect the alkalinity of saline soil and winter wheat growth. *Sci. Total Environ.* **2023**, *866*, 161330.
(28) Elgehama, A. Selective obstruction of the mTORC2 complex by a naturally occurring cholestane saponin (OSW-1) for inhibiting prostate cancer cell growth. *J. Asian Nat. Prod. Res.* **2022**, *24*, 663−672.
(29) Bai, J.; Liu, Z.; Zhang, R.; Song, F. content and Dissolution Characteristics of Trace Elements in Ornithogalum caudatum Ait and Three Anticancer Chinese Herbs. *J. Cap. Med. Univ.* **2009**, *30*, 208−211.
(30) Sheng, W. G.; Ye, J.; Xu, Y.; Wu, J. Quantitative determination of total sterol in Pule'an Tablets by UV spectrophotometry. *China Med. Her.* **2012**, *09*, 8−10.
(31) Patel, R. K.; Patel, J. B.; Trivedi, P. D. Spectrophotometric method for the estimation of total alkaloids in the Tinospora cordifolia M. and its herbal formulations. *Int. J. Pharm. Pharm. Sci.* **2015**, *7*, 249−251.

https://doi.org/10.1021/acsomega.3c02310
ACS Omega 2023, 8, 23889−23900